Journal of Energetic Materials
Publication details, including instructions for authors and subscription information:
http://www.informaworld.com/smpp/title~content=t713770432

Numerical modeling of composite propellant response to drop weight impact

K. P. Duffy[a]; A. M. Mellor[b]
[a] Department of Mechanical Engineering, Vanderbilt University, Nashville, TN [b] Vanderbilt University, Nashville, TN

To cite this Article Duffy, K. P. and Mellor, A. M.(1993) 'Numerical modeling of composite propellant response to drop weight impact', Journal of Energetic Materials, 11: 4, 261 — 291
To link to this Article: DOI: 10.1080/07370659308019712
URL: http://dx.doi.org/10.1080/07370659308019712

NUMERICAL MODELING OF COMPOSITE PROPELLANT RESPONSE TO DROP WEIGHT IMPACT

K.P. Duffy[a] and A.M. Mellor[b], Vanderbilt University, Nashville, TN 37235

ABSTRACT

Finite element analysis is used to study the dynamic response of propellant subjected to drop weight impact. The model of the propellant incorporates varying amounts of ammonium perchlorate (AP) particles to account for stress concentrations due to sample inhomogeneity. The intent of this study is to examine locations which may lead to critical initiation shear stresses such as AP sliding on AP or AP sliding on steel. The initial full AP model used a 60% (by weight) solids loading corresponding to a research propellant formulated for a companion experimental program. Due to the unusually high number of slidelines which are needed to model the friction between the AP particles and surrounding media, the code was not capable of compiling the full model. Other models have been run to examine

---

[a]Graduate Assistant, Department of Mechanical Engineering.

[b]Centennial Professor of Mechanical Engineering.

Journal of Energetic Materials Vol. 11, 261-292 (1993)
Published in 1993 by Dowden, Brodman & Devine, Inc.

the effects of a few AP particles on the resulting stress state in the propellant. These models show significant increases in the maximum shear stress at locations immediately surrounding the AP particles. Quantitative comparisons are also made between homogeneous propellant and AP–in–propellant models. Two–dimensional geometric constraints of the code are also discussed. In particular, it is shown the default axisymmetric and the alternative plane strain geometries have limitations which do not allow for proper modeling of the particles. Finally, the limitations of using hydrocodes for simulating the effects of particles in propellant are discussed along with recommendations for further work.

INTRODUCTION

The high strain rate material behavior determines the sensitivity of a composite solid rocket propellant to drop weight impact. The small scale drop weight impact sensitivity of the material is thought related to the large scale system level response and thus the safety of a solid rocket motor containing that propellant. The micromechanical aspects of the solid propellant during impact are difficult to quantify due to the data acquisition limitations of standard drop weight machines. Dynamic finite element analysis of a standard drop weight impact machine has been performed to provide local estimates of, for example, shear stress and pressure in the propellant. By knowing how these variables are distributed, a better understanding of the mechanisms which lead to ignition is achieved. Current

techniques for using dynamic finite element analysis to model sample deformation in the drop weight test are explained.

Previous modeling has assumed a homogeneous representation of the propellant.[1-3] However, actual solid propellant contains crystalline oxidizer particles, and to properly model the behavior of the deforming propellant, these particles should be included in the binder matrix.

Baker et al.[4] hypothesize that energy localization and initial reaction may occur at the large AP particle locations in composite solid propellant. A description of the stress state on an AP particle is necessary for understanding this ignition mechanism. Thus, the initial goal for the present work was to insert a random distribution of AP particles in the binder matrix, compress this new inhomogeneous propellant, and examine the resulting stress state on individual AP particles. The results of this model could be coupled with hot spot models to obtain a more fundamental understanding of impact initiation scenarios.

In conjunction with the experimental drop weight impact program[4], the hydrodynamic finite element code, DYNA2D, from Lawrence Livermore National Laboratory[5] is used. The present computations are performed on a DEC VAX 8800. DYNA2D is an explicit, central difference, Lagrangian code developed primarily to handle large deformations of energetic materials used in military applications. A comprehensive description of the code is found in Goudreau and Hallquist.[6] A contact/impact algorithm, which allows sliding friction definitions between material interfaces, is implemented in the code as well as rezone capability.[7]

Definition of Model Setup

The axisymmetric finite element grid shown in Fig. 1 models the experimental drop weight machine.[4] At time zero the drop weight and striker are given an initial velocity of 8.4 m/s (corresponding to an experimental velocity). DYNA2D then predicts the time dependent deformation of the sample.

The material properties of the steel and aluminum sections are shown in Table 1. The 0.1 cm thick by 0.25 cm radius propellant sample is modeled

TABLE 1. Material Properties[a] for Present DYNA2D Computations

Material	Elastic Modulus, E_{elas} (dyne/cm^2)	Poisson's Ratio, ν	Density ρ (g/cm^3)	Yield Stress, σ_y (dyne/cm^2)	Plastic Modulus, E_{plas} (dyne/cm^2)
Steel	2.07×10^{12}	0.3	7.8	NA	NA
Al	7.24×10^{11}	0.33	2.7	NA	NA
Binder	6.895×10^{8}	0.499	1.833	6.895×10^{7}	6.895×10^{7}
AP	2.07×10^{11}	0.35	1.95	NA	NA

[a]Values for steel and aluminum taken from Hodgman[8]; values for binder and AP taken from So and Francis[9].

with 10 axial and 25 radial elements resulting in an initial length to diameter ratio (L/D) of 1 where the length of each side is approximately the diameter of a 100 μm AP particle. Following So and Francis[9], an isotropic, linearly elastic, linearly plastic, constitutive material model is used for the binder, and a linear elastic model is used for the AP particles. Properties for the

binder and AP are also given in Table 1. Solid propellant has a Poisson's ratio, ν, of near 0.5. However, using a value too close to 0.5 in the code was expected to lead to computational difficulties because of a term involving $(1-2\nu)^{-1}$ in the constitutive equations.[10]

Random Particle Distribution Generator

First, a method was devised to generate a random distribution of AP particles in the binder matrix. For a propellant loaded to a volume percentage, V, the number of possible permutations, P_{tot}, is calculated as:[11]

$$P_{tot} = M!/(N!\times(M-N)!) \qquad (1)$$

where M is the number of possible locations for an AP particle, and $N=V\times M$.

For the 10×25 (M=250) mesh and a 43% volume loading (typical for an HTPB/AP propellant with a 60% by weight solids loading)

$$P=250!/(108!\times(250-108)!)=9.05\times10^{72} \qquad (2)$$

which is a prohibitively large number of possible distributions.

To account for this problem, FORTRAN programs were written which generate random distributions of AP particle locations in a 10×25 matrix. The first program gives each cell an equal probability of being occupied, and each cell has an equal weighting function. However, the axisymmetric geometry of this problem suggests that cells located near the centerline will occupy significantly smaller volumes than those near the outer edge. Therefore, the second program includes a radial weighting function.

To determine lower and upper bounds to the total number of possible particles, the matrix is filled starting from both the outside and inside. The lower and upper bounds are calculated as 62 and 164 particles, respectively. Numerous seed numbers are used to produce different distributions with a spread of particles ranging from 102 to 113.

As mentioned previously, energy localization may occur near the large AP particles, leading to initiation.[4] From the distributions all possible boundary interactions involving an AP particle are considered where stress concentrations are found: AP/steel, AP/binder, and AP/AP. One of the random distributions is shown in Fig. 2 and was chosen as the particle model input for the DYNA2D simulations since it has a reasonable distribution of the three types of interactions.

RESULTS

Initial Full Scale AP Models and Simplifications

The model is constructed as follows. First, the 250 individual propellant elements are defined as separate entities and given the mechanical properties of either binder or an AP particle (see Table 1) following the distribution map (Fig. 2). When two different materials are in contact with one another, DYNA2D requires that a slideline is defined between them if relative motion is expected; otherwise they must be tied together. Relative motion between the particles or binder and steel surfaces is desired, so to simplify the first

model, only slidelines between the AP and steel, binder and steel, and between adjacent AP particles are defined. A dynamic friction coefficient of $\mu = 0.2$ is used at all interfaces. Results from a simplified axisymmetric three AP particle model (a description of this model is given below) showed no difference in the computed stress state with $\mu = 0.5$ or 0.2 along the AP/steel interfaces. Therefore, in the following cases, $\mu = 0.2$ friction coefficients are used at all AP/steel and binder/steel slidelines. The AP/binder and binder/binder interfaces are tied. Even with these simplifications, over 200 slidelines are defined manually. When DYNA2D attempts to compile the model setup into its executable FORTRAN data file, the compilation fails. The difficulties occur in the implementation of the contact/impact algorithm where the slideline relationships are defined. The code cannot handle the large number of slidelines in such close proximity to one another.

A further simplification is made by only defining slidelines between the AP/steel and binder/steel surfaces and tying all the internal particle and binder elements. This model (see Case A, Table 2) does successfully compile; however, it computes to only 0.75 μs. By 0.5 μs the mesh is completely tangled, and shortly thereafter the computation stops due to nodal mapping problems and penetration of the particles into the steel.

Previous publications include discussion of methods to reduce penetration by adjusting the interface stiffness (STIF) and timestep (TSCL) scaling factors (see e.g., Duffy and Mellor[3]). Cases B and C (Table 2) are attempts to optimize the computation by adjusting these parameters based on results

TABLE 2. Summary of DYNA2D composite runs.[a]

Case	Description	STIF	TSCL	Comp. Time (μs)
A	Full AP loading, AP/steel, binder/steel slidelines	0.1	0.667	0.75
B	same as A, "optimal" STIF, TSCL	1.0	0.2109	0.14
C	same as A, $\downarrow$ STIF	0.01	0.2109	0.58
D	top row of AP particles redefined as binder	0.1	0.667	0.42
E	4 AP model	0.1	0.667	30
F	3 AP model	0.1	0.667	45
G	3 AP moved up 1 row	0.1	0.667	40
H	homogeneous, plane strain, 4×25 propellant mesh	0.1	0.667	75
I	same as F, plane strain geometry	0.1	0.667	50
J	homogeneous, plane strain, 10×25 propellant mesh	0.1	0.667	130
K	same as I, $\mu = 0.5$ at AP/steel interfaces	0.1	0.667	55
L	Same as A, plane strain	0.1	0.667	0.74

[a]Cases A—G use axisymmetric geometry.

obtained for the homogeneous propellant model. However, both adjustments lead to shorter computation times than Case A.

In the next AP model (Case D, Table 2), the top row of five AP particles (see Fig. 2) is redefined as binder, with the remaining rows still AP. This

was done to determine if the penetration is a result of the isolated AP/steel interactions or the combined effect of the large number of hard particles. However, since the computation time was only 0.42 μs, and similar severe penetration at the AP/steel interfaces was observed, no absolute conclusions can be drawn without more modeling variations. At this point in the AP particle modeling, further simplifications were made to determine the effects on computed propellant deformation of a smaller number of particles.

Four AP Particle Model (Case E)

The first reduced particle model was run to verify if penetration of particles on the top row, without the effect of a large number of additional particles, causes the short computation times in the full AP particle models (Cases A through D). A single particle is inserted in the top row of the binder at the outer edge (Fig. 3). The reason for the three AP particles included on the bottom row is explained in the next section. This computation runs to 30 μs, whereafter significant penetration occurs at the top row AP particle (Fig. 4). Still, the >> 1 μs computation time suggests that the problems in the full AP particle model stem more from the large number of particles rather than from isolated AP/steel penetration. The penetration also probably depends on where the fourth particle is located since pressure is a function of radial location. Therefore, a particle located near the centerline will be subjected to greater pressure, and is more likely to penetrate into the steel than one located near the outer edge.

Three AP Particle Model (Case F)

So[12] performed a three AP particle calculation using DYNA2D in which he showed significant differences in the propellant stress state between the case with particles and that for homogeneous propellant. To perform a similar computation and compare the results, the three AP particle model (Case F, Table 2) is constructed by removing the top outer particle from the previous model. Slidelines ($\mu = 0.2$) are defined at the three AP/steel locations and the binder/steel interfaces, and other interfaces are tied. Rezoning commands are applied every 5 μs to disentangle the mesh.

The differences between this model and So's are his assuming a simplified linear elastic representation for the binder elements ($E_{elas} = 3.45 \times 10^8$ dyne/cm^2, $\nu = 0.49$) and his sample mesh having one less element radially. The density of his striker and anvil was artificially inflated to simulate larger masses. Also, no rezone commands were used as evidenced by the hourglassing of the elements in a deforming mesh sequence (not shown).

The model used in this study (Case F) runs to 45 μs before severe penetration occurs. From the deforming mesh sequence (Fig. 5), it is clear the AP particles exhibit no radial motion, the same as in So's results, and the binder is forced to flow over the particles. Contours of pressure at 40 μs show a somewhat distorted pressure field when compared to typical homogeneous results.[1] Also, shear stress concentrations are evident near the AP particles.

So[12] showed that in the presence of AP particles there was, at 40 μs, a

56% increase in i–j shear stress (along radial axis) over homogeneous model results at the element immediately to the left of the middle AP particle. Also, a 36% increase occurred in the element to the left of the outermost AP particle. The results from the present study indicate similar particle effects but with increases of 32% and over 200% near the middle and outer particles at 40 μs, respectively. These differences arise from the model inconsistencies mentioned earlier, as well as from the oscillations in the stress–time curves, but both results show the same qualitative increase in shear stress with the inclusion of particles.

Two reasons are postulated for the negligible motion of the AP particles mentioned earlier. The first may stem from the penetration/interface stiffness relationship mentioned earlier. The higher particle modulus leads to an increased stiffness at the 3 AP/steel interfaces. This, in turn, results in slightly more penetration which inhibits the radial expansion. The second reason lies in the large circumferential stresses resulting from the axisymmetric geometry (discussed later). The former hypothesis led to a model in which the 3 AP particles are moved up one row vertically so that no AP/steel interfaces exist, but binder/steel slidelines are still defined.

Three AP Particles Moved Vertically Up One Row (Case G)

An initial calculation in which slidelines ($\mu = 0.2$) were defined at the particle/binder interfaces produced unrealistic results when the binder flowed radially through the particles after 10 μs. Thus, in a new model, the

particles and binder were tied together allowing no relative motion between them. This calculation is terminated at 40 μs due to severe penetration. The maximum shear stress contours show a significant stress concentration at locations adjacent to the particles. The binder still is stretched around the particles, and as in Case F, they do not appear to move radially. The penetration of the particles into the steel has been eliminated, and the radial motion is still inhibited; thus, the primary reason for this inability to move must lie in the model geometry. Since an axisymmetric geometry is used, the particles are actually square annuli. The high AP particle modulus relative to the softer binder modulus prohibits radial motion, and large hoop stresses build up. The alternative geometry available in DYNA2D is plane strain where a two–dimensional object is assumed to have an infinite depth into the plane of the paper. However, before studying the effects of plane strain geometry on the particle model, comparisons are first made with the simplified homogeneous models used in earlier studies.

Plane Strain Homogeneous Model (Case H)

A model was constructed in which all the elements were given binder mechanical properties. The resulting computation in plane strain geometry with the 4×30 homogeneous propellant mesh (Case H) ends at 75 μs and has a different propellant stress state than the axisymmetric geometry. The pressure in the middle bottom element is approximately 20% higher over time in the plane strain model. The discrepancies at times greater than 60 μs

result from slight penetration in the plane strain model which does not occur in the axisymmetric model. The maximum shear stress over time for this same element location exhibits a similar trend (about 25% higher for the plane strain case). Thus, the infinite depth assumption of the plane strain geometry results in higher stresses over the same time interval than in the axisymmetric geometry. The 20–25% difference held for other locations examined in the propellant as well, and this difference should be taken into account when making any stress state comparisons between the two models. Next, the plane strain geometry is applied to the particle model to allow for more unconstrained radial expansion.

Plane Strain AP Particle Model (Case I)

The three particle model with the AP on the bottom row is used. All conditions are identical to Case F except for the plane strain geometry. Smoother deformation results than for the axisymmetric geometry with significantly less binder stretching around the particles (Fig. 6). Also, the two outer particles move away from the centerline permitting the computation to proceed to 50 μs before penetration begins. The resulting stress state using the plane strain geometry in the particle model is different from the axisymmetric geometry results. The pressure distribution is similar to the axisymmetric geometry, especially at later times with no noticeable increase over the axisymmetric results. However, the lessened radial constraint as a result of the plane strain geometry is evident from shear

stress contours where a more uniform shear stress distribution results at later times compared to the axisymmetric geometry.

Comparison Between Homogeneous and Particle Models

To quantify some of the previous conclusions concerning the effects of solid particles in the models, comparisons using the axisymmetric geometry are made between the homogeneous and 3 AP particle models (Case F, Table 2). Similar comparisons are made using the plane strain geometry. Since the only plane strain particle model to this point used a 4×30 propellant mesh (Case I), a new case (J) was run with identical specifications as Case I without particles and a 10×25 propellant mesh is used.

The elements compared are in the vicinity of the particles as shown in Fig. 7. At a location near the centerline (266 (homogeneous) and 478 (AP)), the resulting maximum shear stress over time is similar for both axisymmetric cases. Near the middle of the propellant (277 (homogeneous) and 488 (AP)), the presence of the particle results in a 15% increase in maximum shear stress at any instant in time. Particle effects become even more important near the high shear outer edge region (288 (homogeneous) and 498 (AP)). Figure 8 shows a 67% increase at 45 μs in the maximum shear stress near the outer edge location when the AP particle is adjacent to this location. Similar results are found at the element located directly above the particle.

The presence of particles is nearly insignificant when using the plane strain geometry. At the same centerline location, the maximum shear stress

over time is also not affected by the presence of an AP particle. At the middle location the increase in shear stress with the particle in the mesh is also negligible. Finally, near the outer edge location, the shear stress curves overlap except at oscillation points in the homogeneous curve.

The fact that the inclusion of particles in a plane strain geometry results in no significant difference compared to the homogeneous model is a cause for concern. Conceptually, the hard particles should slow the radial expansion and allow larger stresses to build. The explanation for this discrepancy lies in the friction coefficients chosen at the AP/steel and binder/steel interfaces. Both these values were set to 0.2 because an earlier study showed no differences in the computed deformation and stress state for an axisymmetric particle model in which the AP/steel dynamic friction coefficient was changed from 0.2 to 0.5. However, that result was due more to the axisymmetric geometry which inhibits the radial expansion of the particles and dominates any effects which the increased friction coefficient might have had. To test this theory the AP/steel friction coefficient in the plane strain particle model (Case I) was increased to 0.5 leaving the binder/steel coefficient at 0.2. Using the 0.5 value is an assumption since the dynamic friction coefficient between AP and steel is not known. However, the value is expected to exceed that for the binder/steel interface. This case (K) had a similar computation time and deformation history to Case I, but upon closer inspection, the effects of the increased friction coefficient are manifested.

Time history plots (Fig. 9) of the radial expansion at three binder nodes adjacent to the particles (see Fig. 7) indicate an overall decrease when the

higher friction coefficient is used. At 30 μs an average radial expansion decrease of 15% is observed for the three locations. Since these curves appear to diverge over time, the effect of the increased friction coefficient would be even more significant near the experimental ignition time of 150 μs.

When the Case K results are compared with the $\mu = 0.2$ maximum shear stress curves, the effects of increasing the AP/steel friction coefficient are evident. Though the centerline location is not affected, at the other locations, an approximately 10% increase in maximum shear stress occurs when the higher friction coefficient is used with the plane strain geometry.

Particle Modeling Conclusions

The reduced particle plane strain models had longer computation times compared to their axisymmetric counterparts since the large hoop stresses were eliminated. The reason the models were scaled back from the initial particle distribution is because the large number of particles resulted in an extremely hard sample which caused severe penetration problems and limited computation times to under 1 μs. A final verification of this explanation is made by using a plane strain geometry with the fully loaded sample (Case L). If the constraints imposed by the axisymmetric geometry are removed, and a significantly longer computation time results, then the large hoop stresses would be responsible for the computation problems. The particle distribution for this model was generated with the FORTRAN program which did not include a radial weighting function. Since a plane strain

geometry is now used, the weighting function is not necessary. As Table 2 indicates, no increase in computation time occurred. The deforming mesh sequence (not shown) is nearly identical to the Case A axisymmetric results. These results prove that, while the plane strain geometry permits significantly longer computation times in the reduced three particle models, no similar improvements result when this change is applied to the full particle distributions.

The implications of this result are discussed in the conclusions. The results illustrate that even state–of–the–art two–dimensional dynamic hydrocodes, like DYNA2D, are not fully capable of simulating the impact of large distributions of solid particles in soft binder material out to significant computation times using the simplifying geometric assumptions made in both the axisymmetric and plane strain models. Even still, reduced particle models have shown the effects of a small number of these particles and have added insight into the drop weight impact propellant deformation process. The computed stress state differences when only a few annular (axisymmetric) or longitudinal (plane strain) particles are included in the model indicate their effects cannot be ignored. The presence of these particles results in increased values of shear stress at locations in their vicinity. This effect is even more pronounced near the outer edge of the sample. Clearly, the particles affect the stress state in a manner which would tend to validate the findings of Coffey and Armstrong[13], who observed hot spot formation at the highly sheared outer edge of the sample.

CONCLUSIONS AND FUTURE EFFORTS

Several techniques are currently used to model the response of energetic material subjected to various stimuli. The accuracy of these simulations is limited by, among other submodels, the constitutive relations used to describe the component material behavior. For elastic materials such as steel, these relations and the corresponding constants are well–understood. However, for energetic materials, the behavior is more complicated. For small displacements and/or low strain rates, simplifying assumptions make the problem tractable to model in a finite element code. But for large displacement and/or high strain rates, typically found in tests such as drop weight impact, accurate material property characterization of the energetic material is required over the entire sample deformation time since different modes of failure occur at different rates. This information is now becoming available due in large part to research efforts in the solid rocket and gun propellant communities.

The composite models are the only finite element models known which attempt to determine effects of solid particles on the deformation and stress state of a polymeric binder. The results indicate a two–dimensional code, like DYNA2D, has limited capability to model such a situation. When a distribution of particles, typical of a highly loaded solid rocket propellant, is included in the model, the computation does not proceed longer than 1 μs which is at least two orders of magnitude short of the desired time to allow reasonable comparison with drop weight experiments. The problems stem

from the numerous required slideline definitions between adjacent moving parts which even the state–of–the–art DYNA2D algorithms cannot handle.

Accepting this fact, scaled–down three particle models were constructed and indicate that even a small number of particles has a significant effect on the sample stress state. It is shown that the default axisymmetric geometry does not allow for proper modeling of the particles because, in this geometry, what appears in the 2–D frame of reference as a square particle is really an annular particle. A large hoop stress builds in this annulus due to its high yield point and radial constraint, which severely alters the computed stress state and leads to unwanted numerical difficulties such as penetration and mesh entanglement. Using the alternative plane strain geometry, which models the annular particles as infinite particle strips, reduces the magnitude of these problems but is still an oversimplified assumption.

One suggestion for further work with the composite model is to use the orthotropic–elastic constitutive material model in DYNA2D for the three particles. Here, elastic modulus and Poisson's ratio values are defined differently for both the axial and radial directions. Using a lower radial elastic modulus would permit more radial deformation and might overcome the difficulties encountered previously with the axisymmetric particle models.

Whirley[14] recently indicated that the slideline algorithms, which limited the 2–D fully–loaded propellant calculations, have been improved in the three–dimensional hydrocode, DYNA3D. A 3–D simulation of the drop weight impact test with a composite propellant sample might produce better

results than previously obtained. In this case the two–dimensional geometric constraints would be removed. This would probably allow a three particle model to compute to significantly longer times, but will only indicate more quantitatively what is already known qualitatively: that even a small number of particles has an effect on the resulting propellant stress state. The significant increase in cost to reach that conclusion is not justifiable. Furthermore, the initial intent of the composite models was to show the effects of particles in a typically–loaded propellant which has thousands of particles in a sample of the size used in the drop weight impact test. Even the improved slideline algorithms of DYNA3D (actually slide surfaces) will most certainly not handle such a large number of interface definitions. This number is further increased since a 2–D geometry requires only four slideline definitions for the four sides, but the 3–D box particle requires six surface definitions.

Even if algorithm advancements someday make this problem tractable, the fact that the solution is only as good as the accuracy of the material model is a reality that cannot be ignored. Since engineering/constitutive relations will undoubtedly continue to see use in finite element codes, the need for accurate high rate mechanical properties will continue. However, the current implementation of these non–linear viscoelastic constitutive relations in hydrocodes severely limits their use in modeling high rate tests such as drop weight impact since the applicability of the model constants does not extend outside the limited rate range in which they are usually obtained. The efforts of Lieb and Leadore[15 and 16] and others will help to

extend this range.

A molecular–based model[17] shows promise since it does not rely on large amounts of experimental data as do the constitutive models. The advances in computing capability now make this a plausible material modeling technique. However, the effects of rate and/or temperature must be properly added to the model, and future funding would be more properly directed to that area.

The results indicate the limit of dynamic finite element codes has been reached for use as a purely mechanical model without a detailed hot spot/ignition model. When modeling tests such as drop weight impact in which the energy is localized as hot spots, the simulations can never correctly predict ignition unless detailed energy localization schemes are incorporated in the models. The shear banding model of Baker and Mellor[18] and the Johnson et al.[19] and Kang et al.[20] hot spot models are examples of energy localization models which eventually could be implemented into hydrocodes like DYNA2D. These types of models will give an increasingly more realistic view of the ignition process for energetic materials subjected to impact.

ACKNOWLEDGEMENTS

This work was performed under Contract DAAL03–89–K–0061 with the Army Research Office (Contract Monitor, D.M. Mann). The views, opinions and/or findings contained in this paper are those of the authors and should not be construed as an official Department of the Army position, policy, or

decision, unless so designated by other documentation.

REFERENCES

1. Duffy, K.P., Master's Thesis, Mechanical Engineering, Vanderbilt University, Nashville, 1993.

2. Duffy, K., Baker, P., Barr, E. and Mellor, A., AIAA Paper 91–2193, 27th Joint Propulsion Conference, Sacramento, 1991.

3. Duffy, K.P. and Mellor, A.M., "A numerical study of drop weight impact testing of solid rocket propellants," Tenth Symposium (International) on Detonation, Boston, MA, (1993).

4. Baker, P.J., Mellor, A.M. and Coffey, C.S., *J. Propuls. Power* 8:3, 578 (1992).

5. Hallquist, J.O., "User's manual for DYNA2D," Univ. of Cal., Lawrence Livermore National Laboratory, Report UCID–18756, Rev. 1, (1982).

6. Goudreau, G.L. and Hallquist, J.O., *Computer Methods in Applied Mechanics and Eng.* 33, 725 (1982).

7. Hallquist, J.O., in Computational Techniques for Interface Problems, K.Park and D. Gartling, eds., A.M.D. Vol. 30, ASME, United Engineering Center, New York, 1978.

8. Hodgman, E.C., Handbook of Chemistry and Physics, 42nd Edition, The Chemical Rubber Publishing Co., Cleveland, 1961.

9. So, W.T. and Francis, E.C., J. Spacecraft & Rockets 28, 658 (1991).

10. Francis, E.C., United Technologies, Chemical Systems Division, Personal Communication, 1990.

11. Incropera, F.P., Introduction to Molecular Structure and Thermodynamics, Appendix B, Wiley & Sons, New York, 1974.

12. So, W.T., "Dynamic finite element analysis of drop weight impact test of solid propellant," United Technologies, Chemical Systems Division, Internal Report, 1991.

13. Coffey, C.S. and Armstrong, R.W., in Shock Waves and High Strain–Rate Phenomena in Metals, Plenum, New York, 1981, p. 313.

14. Whirley, R.W. (1993), Lawrence Livermore National Laboratory, Personal Communication.

15. Lieb, R. and Leadore, M., "Mechanical response comparison of gun propellants evaluated under equivalent time–temperature conditions," JANNAF Structures and Mechanical Behavior Subcommittee Meeting, Albuquerque, NM, 1992.

16. Lieb, R. and Leadore, M., JANNAF Propulsion Systems Hazards Subcommittee Meeting, CPIA Publ. 582, Vol. I, 1992, p. 145.

17. Davis, I.L., Thiokol Corporation, Personal Communication, 1990.

18. Baker, P.J. and Mellor, A.M., AIAA/SAE/ASME/ASEE 28th Joint Propulsion Conference, AIAA Paper 92–3631, Submitted to J. Prop. Power, 1992.

19. Johnson, J.N., Tang, P.K. and Forest, C.A., Eighth Symposium (International) on Detonation, NSWC MP 86–194, 1985, p. 52.

20. Kang, J., Butler, P.B. and Baer, M.R., *Combust. Flame* 89, 117 (1992).

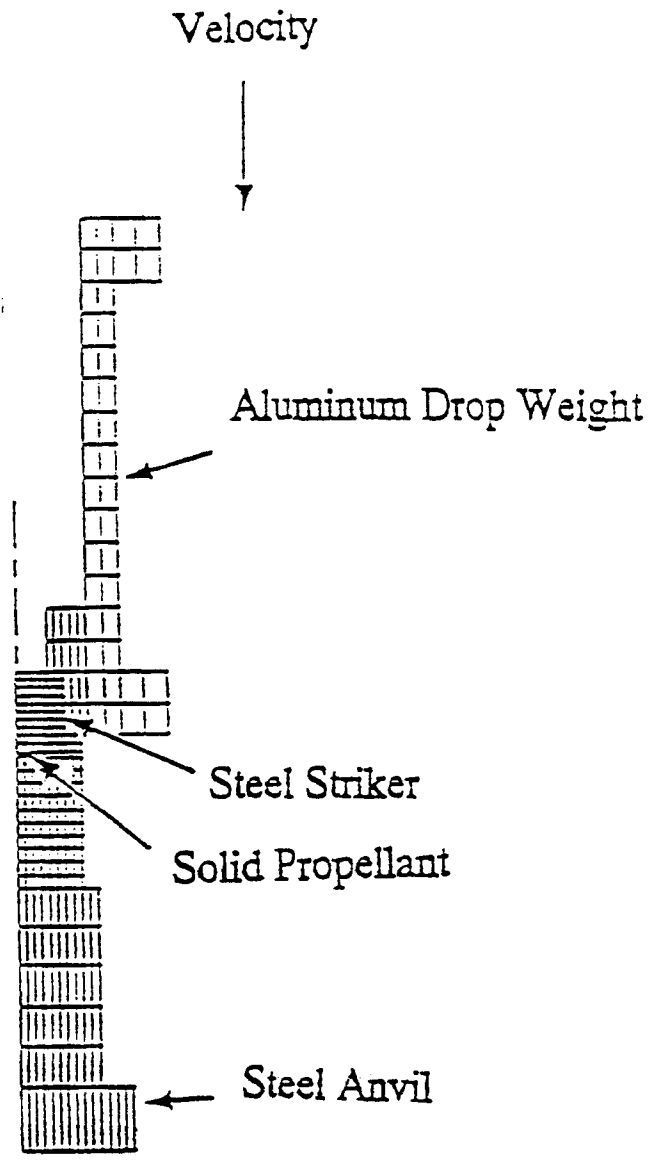

FIGURE 1
DYNA2D mesh of the drop weight impact machine. Length from top of drop weight to bottom of anvil is 19 cm.

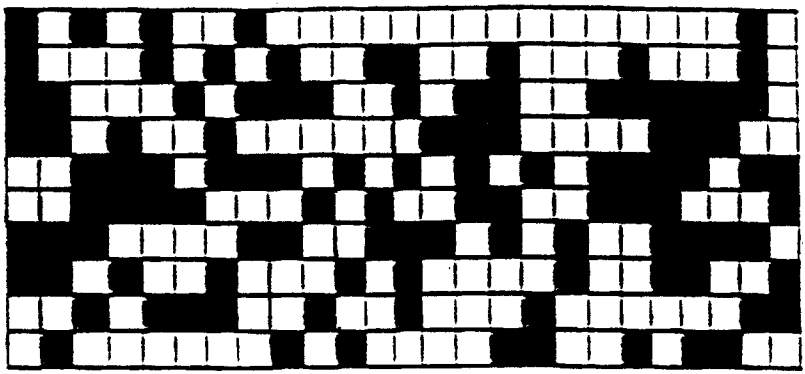

FIGURE 2
Random particle distribution chosen for the model. Particle locations shown in black.

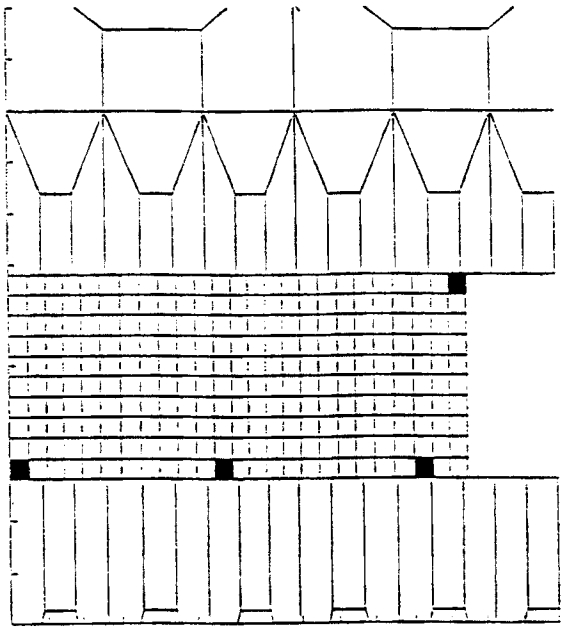

FIGURE 3
Expanded view of propellant mesh showing location of four AP particles (Case E).

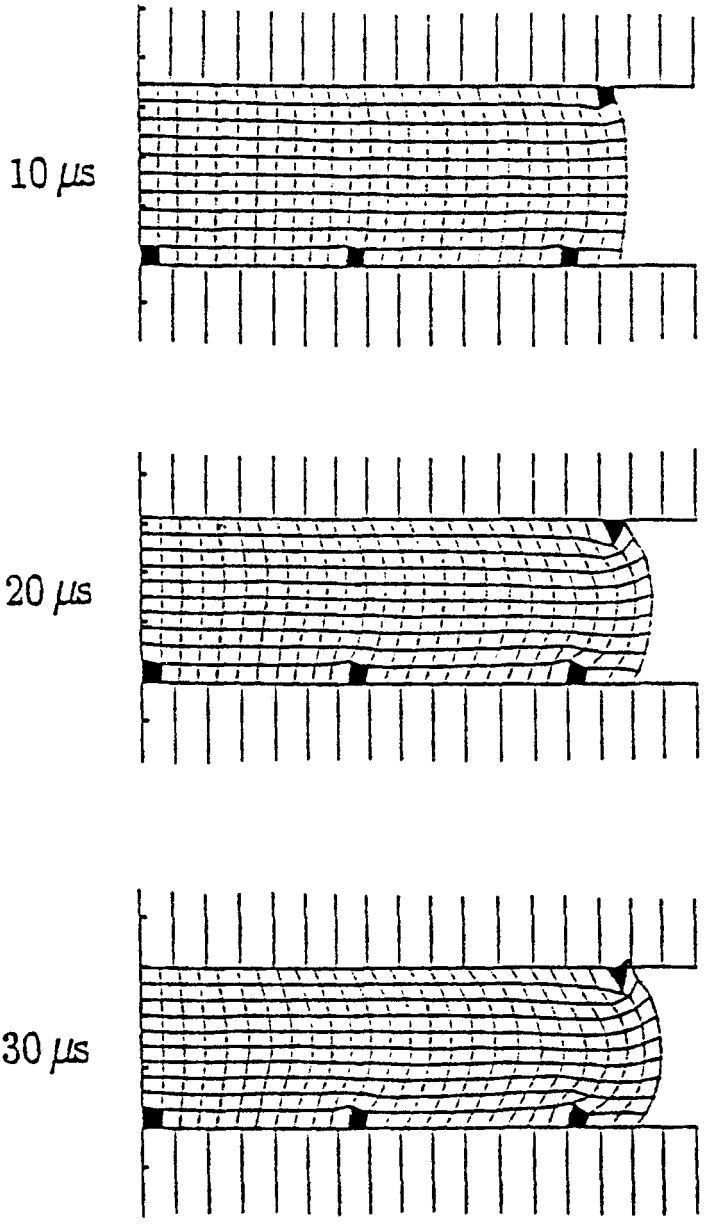

FIGURE 4
Propellant compression profiles for Case E.

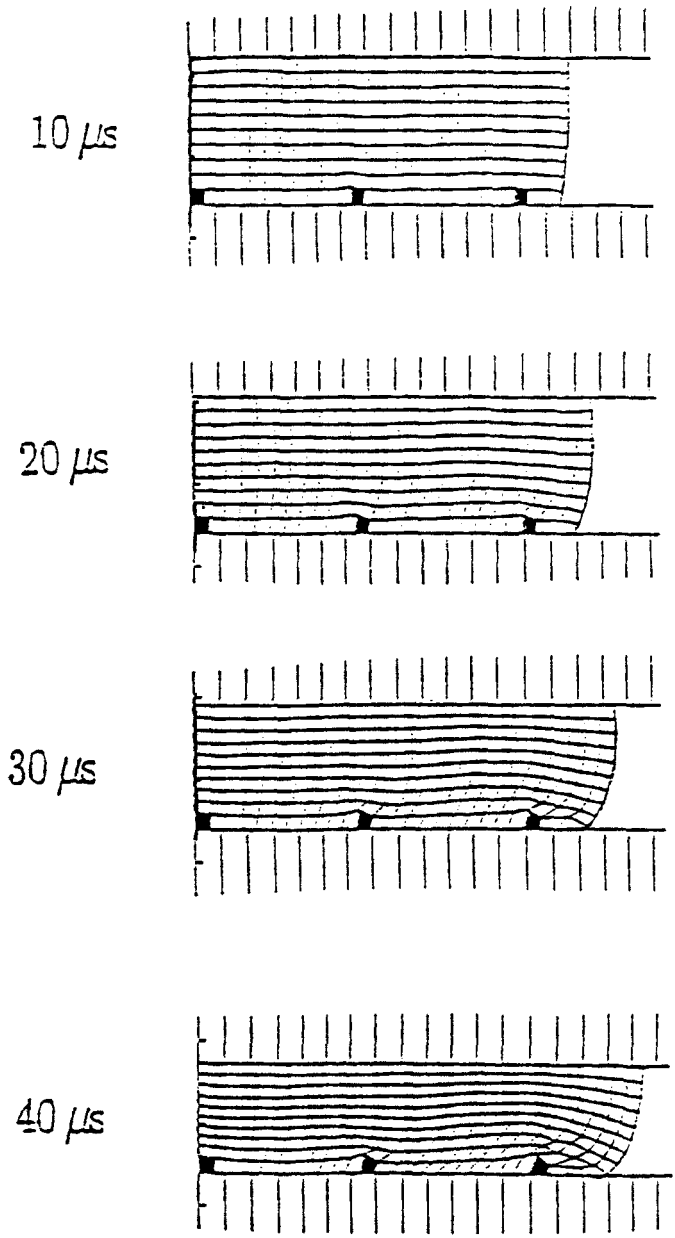

FIGURE 5
Propellant compression profiles for Case F.

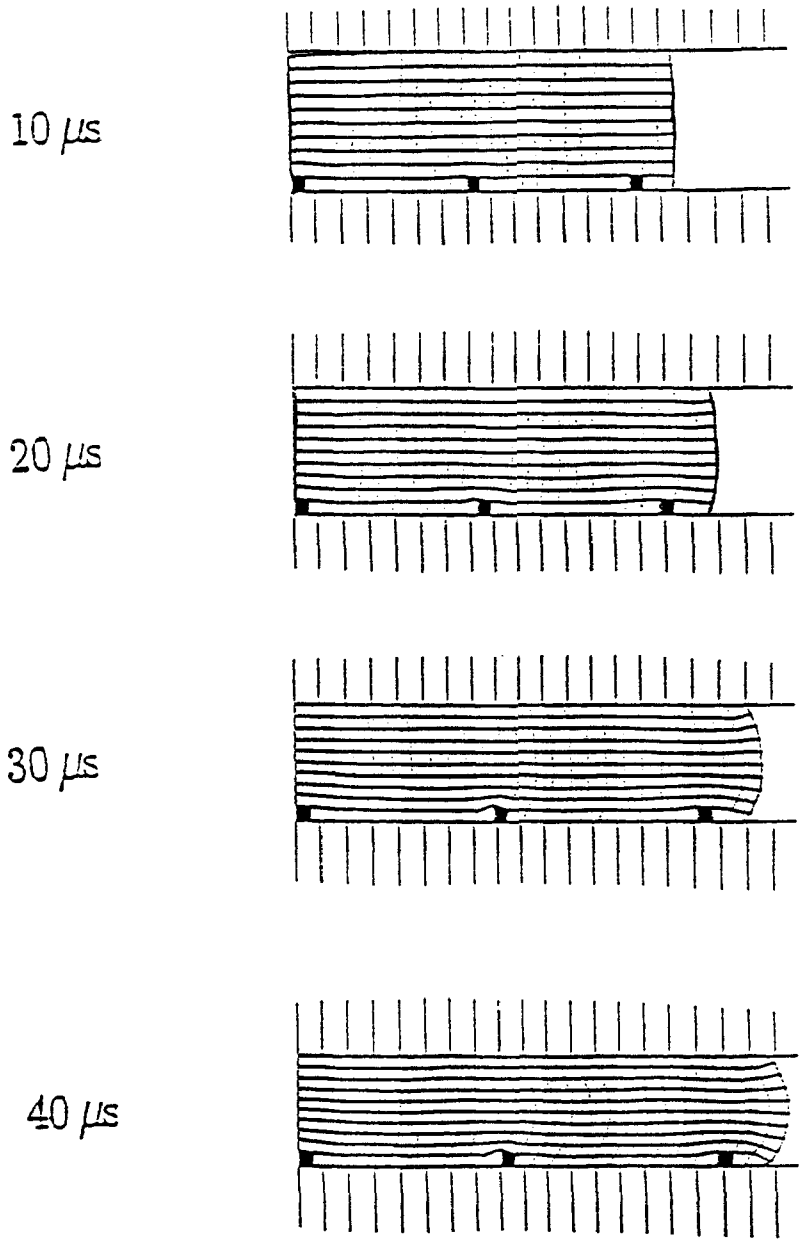

FIGURE 6
Propellant compression profiles using plane strain geometry (Case I).

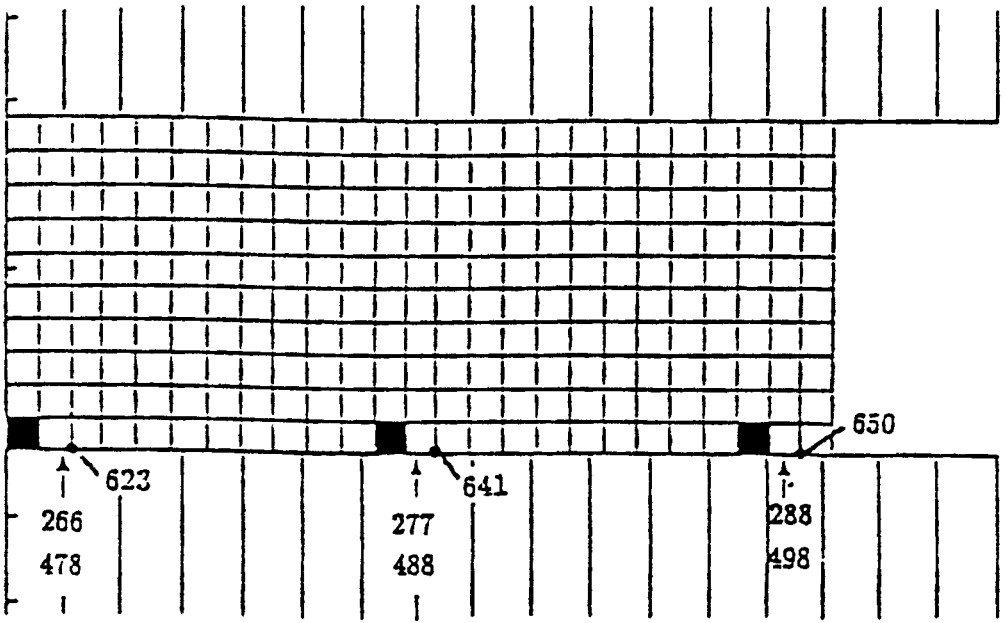

FIGURE 7
Elements and nodes examined in homogeneous/AP particle comparisons.

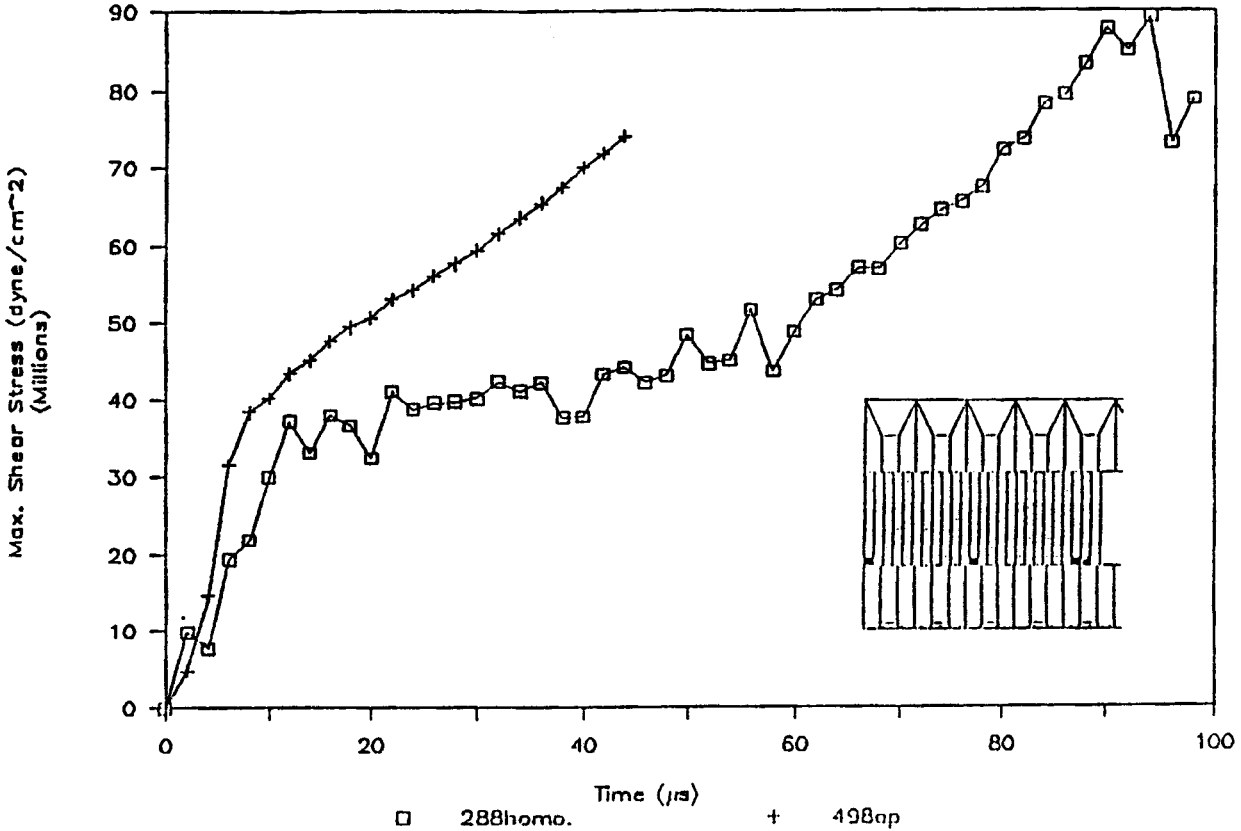

FIGURE 8
Maximum shear stress versus time for near edge element, axisymmetric geometry.

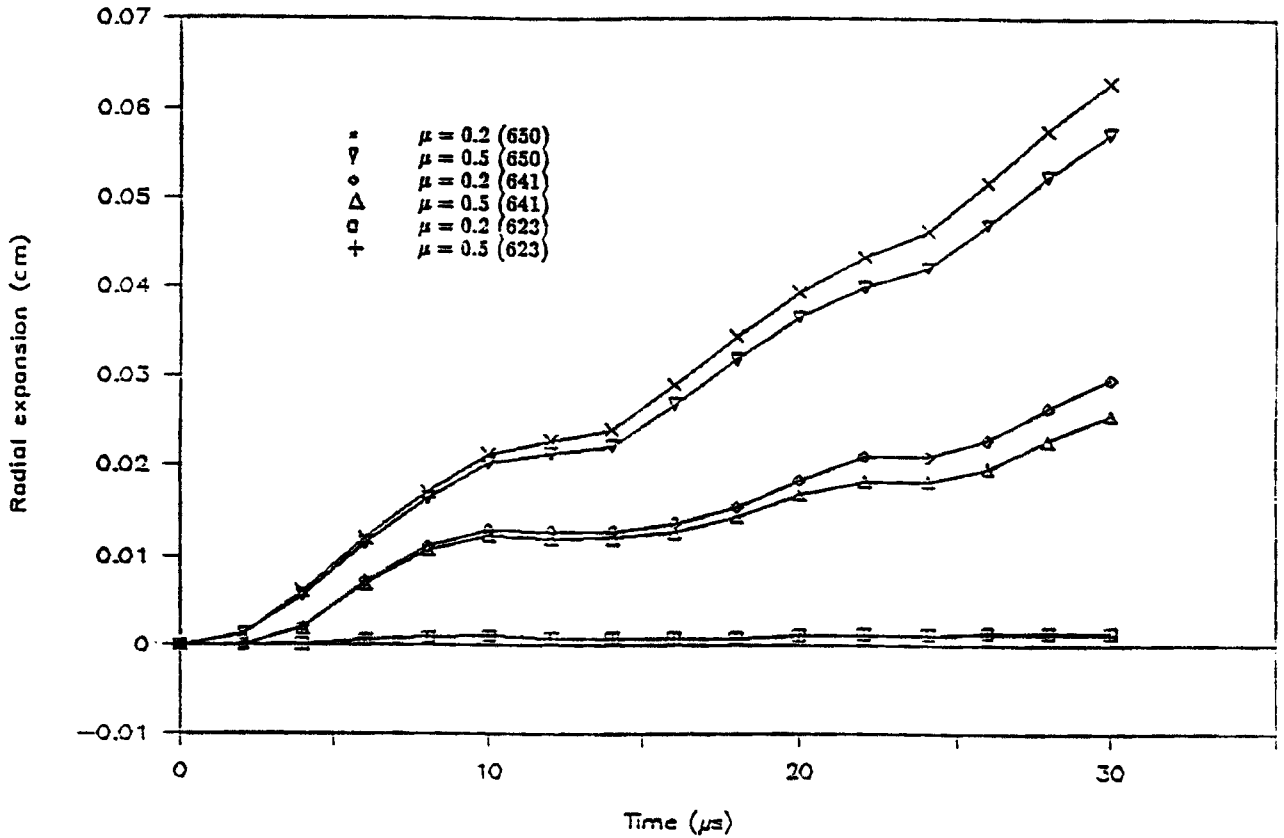

FIGURE 9
Radial expansion at nodes 623, 641 and 650 for $\mu = 0.2$ and 0.5 AP/steel friction coefficients.